

*Temporary address.

¹E. M. Conwell, in *Solid State Physics*, edited by F. Seitz, D. Turnbull, and H. Ehrenreich (Academic, New York, 1967), Suppl. 9, p. 14.

²H. Fröhlich and B. V. Paranjape, Proc. Phys. Soc. (London) **B69**, 21 (1956).

³R. Stratton, Proc. Roy. Soc. (London) **A242**, 355 (1957); *International Conference on Solid-State Physics, Brussels, June, 1958* (Academic, New York, 1960), Vol. I, p. 343.

⁴A. Hasegawa and J. Yamashita, J. Phys. Soc. Japan **17**, 1751 (1962).

⁵E. deAlba and V. V. Paranjape, Phys. Letters **11**, 12 (1964).

⁶P. Butcher and W. Fawcett, Proc. Phys. Soc. (London) **86**, 1205 (1965); Phys. Letters **21**, 489 (1966).

⁷E. M. Conwell and M. O. Vassel, Appl. Phys. Letters **9**, 411 (1966).

⁸J. G. Ruch and G. S. Kino, Appl. Phys. Letters **10**, 40 (1967).

⁹B. Fay and G. S. Kino, Appl. Phys. Letters **15**, 337 (1969).

¹⁰A. Sher and K. K. Thornber, Appl. Phys. Letters **11**, 3 (1967).

¹¹A. D. Boardman, W. Fawcett, and H. D. Rees, Solid State Commun. **6**, 305 (1968).

¹²Reference 1, p. 59 ff.

¹³Reference 1, p. 150.

¹⁴Equation (6) is a special form of the Pauli master equation, used extensively in the quantum mechanics of

the solid state. For example, it has recently been used in a theoretical study of transport in asymptotically high magnetic fields perpendicular to electric fields by H. F. Budd, Phys. Rev. **175**, 241 (1968).

¹⁵W. Zawadzki, in *Physics of Solids in Intense Magnetic Fields*, edited by E. D. Haidemenakis (Plenum, New York, 1969), p. 301.

¹⁶V. S. Titeica, Ann. Phys. (Paris) **22**, 129 (1935).

¹⁷P. N. Argyles, J. Phys. Chem. Solids **4**, 19 (1958).

¹⁸V. V. Paranjape and T. P. Ambrose, Phys. Letters **8**, 223 (1964); V. V. Paranjape and E. de Alba, Proc. Phys. Soc. (London) **85**, 945 (1965).

¹⁹B. Magnusson and P. Weissglas, Microwave Dept., Royal Inst. Technology, Stockholm, Sci. Report No. 18, 1967 (unpublished).

²⁰*Handbook of Mathematical Functions*, edited by M. Abramowitz and I. A. Stegun, National Bureau of Standards, Appl. Math. Series 55 (U. S. GPO, Washington, D. C., 1964), p. 376.

²¹M. Sato, J. Phys. Soc. Japan **14**, 1275 (1959).

²²R. Barrie and R. R. Burgess, Can. J. Phys. **40**, 1056 (1962).

²³R. Stratton, Proc. Roy. Soc. (London) **A246**, 406 (1958).

²⁴K. Blötekjaer, Arkiv Fysik **33**, 105 (1966).

²⁵Reference 1, p. 138 ff.

²⁶V. L. Gurevich and Yu. A. Firsov, Zh. Eksperim. i Teor. Fiz. **40**, 198 (1961) [Soviet Phys. JETP **13**, 137 (1961)]; **47**, 734 (1964) [**20**, 489 (1965)].

Electrical Properties of the GaAs X_{1C} Minima at Low Electric Fields from a High-Pressure Experiment

G. D. Fitt and J. Lees

Standard Telecommunication Laboratories Limited, London Road, Harlow, Essex, England
(Received 30 March 1970)

Hall-effect measurements at pressures extending to 60 kbar were made on single crystals of n -type GaAs grown by liquid epitaxy, vapor epitaxy, and bulk techniques over the carrier-concentration range 10^{13} – 10^{19} cm^{-3} and with Se, Si, Sn, and Te dopants. The X_{1C} Hall mobility at 50 kbar for material in the 10^{14} – 10^{17} – cm^{-3} range was 375 ± 45 cm^2/V sec after transfer from the Γ_{1C} minimum. [The labeling of states follows the notation of Wigner where the added subscripts C (as used in X_{1C}) and V (used in Γ_{15V}) refer to conduction- and valence-band states, respectively.] Extrapolation to atmospheric pressure gives a conductivity mobility of 328 ± 50 cm^2/V sec. Theoretical fits for the high-pressure data indicate a subband gap (X_{1C} – Γ_{1C}) of 0.38 ± 0.01 eV and a density-of-states ratio of $(N_x/N_T)_{P=0} = 45$, which implies X_{1C} density-of-states effective mass of $(0.85 \pm 0.10)m_e$. The loss of carriers at high pressures to impurity levels associated with the X_{1C} minima has been observed. The activation energies relative to the X_{1C} minima are estimated at 0.045 ± 0.01 eV for 10^{17} – cm^{-3} material with Si, Se, Te doping. Results have been analyzed in terms of the simple hydrogenic model. Ionized-impurity scattering in the X_{1C} minima has been shown to be unimportant for material with carrier concentrations below 10^{17} cm^{-3} .

I. INTRODUCTION

High-pressure experiments^{1,2} were instrumental in determining the physical mechanism of the Gunn effect in GaAs. The threshold field for Gunn oscil-

lations was found to decrease as the light-effective-mass Γ_{1C} [000] conduction band moved towards the heavy-effective-mass X_{1C} <100> conduction-band minima with pressure. This showed that the negative differential resistance which occurs near 3 kV/

cm in n -type GaAs resulted from the transfer of electrons at high electric fields from the high-mobility Γ_{1C} minimum to the low-mobility X_{1C} minima situated approximately 0.4 eV higher in energy.

The electrical properties of electrons in the X_{1C} GaAs minima are largely unknown. It has been general practice to base Gunn-effect calculations on parameters obtained from GaP and Si, where electrons occupy the $\langle 100 \rangle$ minima at atmospheric pressure. The properties of these electrons at high fields have been calculated by using the observed velocity-field curve to derive the effect of electric field on the different scattering mechanisms. These scattering mechanisms in Si are reasonably well known, but acoustic-mode and equivalent intervalley scattering predominate in this nonpolar material, whereas in GaAs and GaP it is expected that longitudinal-optical polar scattering as well as equivalent intervalley scattering is important.

The highest mobility³ known to us in n -type GaP is 220 cm²/V sec for a carrier concentration near 10¹⁶ cm⁻³ at room temperature. At higher impurity concentrations, the mobility can drop to very low values, typically 40 cm²/V sec. The problem of scattering in GaP, however, is still largely unsolved. Hilsum and Welborn⁴ have predicted theoretically that intervalley scattering will be the dominant mechanism for the X_{1C} satellite valleys. There is little doubt that the principal reason for the confused state of current thinking on scattering in GaP stems from the lack of good-quality homogeneous material.^{5,6}

An alternative method of determining the GaAs $\langle 100 \rangle$ parameters would be to study GaAs/P alloys, but the same argument of poor-quality material applies and hydrostatic measurements by us give mobilities less than 50 cm²/V sec. It was decided, therefore, that the best approach would be to analyze the high-purity GaAs, which is now available, using high-pressure Hall techniques, even though the pressures (~60 kbar) needed meant that solid-pressure transmitting media were desirable.

This paper describes measurements made on GaAs single crystals over the impurity concentration range 10¹³–10¹⁹ cm⁻³ using donor impurities of Se, Si, Sn, and Te. The mobility of electrons in the $\langle 100 \rangle$ minima has been determined experimentally for the first time, with account being taken of carrier "freeze out" to impurity levels associated with the X_{1C} minima. Previous values obtained from simple resistivity pressure curves^{7,8} allow the carrier loss with pressure to be only roughly estimated. By fitting the data to a simple two-band model, incorporating $\langle 100 \rangle$ impurity levels, we have been able to determine values for the Γ_{1C} - X_{1C} subband energy gap, the X_{1C} -minima effective mass, and the excitation energy of impurity levels which lie below the X_{1C} minima but above the Γ_{1C}

minimum. The results are simply analyzed in terms of the most probable dominant scattering mechanisms.

II. BAND STRUCTURE OF GaAs AT HIGH PRESSURES

At atmospheric pressure, it is now well established from experiment and theoretical calculations that the lowest conduction-band minimum in GaAs is at the central Γ point of the Brillouin zone. The effective mass m_F^* at the bottom of the band has been measured recently at room temperature as 0.064 m_e by Faraday rotation,⁹ 0.065 m_e by magnetophonon oscillations¹⁰ and cyclotron resonance,¹¹ and 0.067 m_e by the interband magneto-optical effect.¹² The variation of the effective mass as a function of the forbidden energy gap E_g (1.52 eV at $T=0^\circ\text{K}$) is given by $\vec{k}\cdot\vec{p}$ theory, provided the spin-orbit splitting Δ (0.35 eV) is small compared with E_g . We have

$$\frac{1}{m_F^*} = \frac{1}{m_e} \left[1 + \frac{2m_e M}{3\hbar^2} \left(\frac{2}{E_g} + \frac{1}{E_g + \Delta} \right) \right], \quad (1)$$

where M is the momentum-matrix element between the Γ_{1C} conduction and Γ_{15V} valence states. At high pressures, the Γ_{1C} minimum moves relative to the Γ_{15V} valence band such that E_g increases at a rate near $+10 \times 10^{-6}$ eV/bar. This coefficient is characteristic for the Γ_{1C} minimum in other III-V compounds. Thus, we would expect the Γ_{1C} effective mass to increase with pressure from (1) provided M and Δ are constant, resulting in a decrease in mobility, the magnitude of which will depend on the dominant scattering mechanism.

The energy of the X_{1C} minima above the Γ_{1C} minimum has been generally accepted as 0.36 eV for Gunn-effect calculations following Ehrenreich's¹³ analysis of high-temperature Hall measurements. Hilsum¹⁴ later adjusted Ehrenreich's subband gap to 0.33 eV at room temperature. This would agree with the result obtained by Spicer and Eden¹⁵ from photoemission studies. That the minima should have X_1 rather than X_3 symmetry followed from the group-theoretical arguments of Birman *et al.*¹⁶ James *et al.*¹⁷ have obtained the L_{1C} and X_{3C} minima, respectively, at 0.09 and 0.58 eV above the X_{1C} minima.

The effective mass of the ellipsoidal X_{1C} minima has not been measured directly for GaAs. Ehrenreich suggested a density-of-states effective mass¹³ of 1.2 m_e , and this has been generally accepted for Gunn calculations, perhaps because it agrees with the values for the $\langle 100 \rangle$ minima in Si and GaP, assuming that there are six minima situated at Δ_{1C} points in from the zone edge. Theoretical calculations¹⁸ for GaAs, however, indicate that the X_{1C} minima lie at the zone edge and are three in number.

At high pressures, it is found that the X_{1C} minima move slowly towards the valence band at about

-1×10^{-6} eV/bar, which is consistent with results for GaP and Si.¹⁹ We expect, therefore, to observe the transfer of electrons from the Γ_{1C} to X_{1C} minima near 35 kbar when the minima are equal in energy. The L_{1C} $\langle 111 \rangle$ minima in Ge have a coefficient of $+5 \times 10^{-6}$ eV/bar,¹⁹ and it is convenient to assume that in GaAs the movement will be approximately the same. This assumption was found to be adequate in the analysis of high-pressure GaSb results.^{20,21}

III. SCATTERING OF ELECTRONS AT HIGH PRESSURES

The dominant scattering mechanism in the central Γ_{1C} minimum at low fields is polar-optical (PO) scattering. Ehrenreich¹³ found that the electrical properties over the impurity concentration range 10^{14} – 10^{18} cm⁻³ at room temperature could be explained in terms of combined polar-optical and ionized-impurity (I) scattering. The total mobility according to Ehrenreich is of the form

$$\mu_{I+PO} = [A T^{1/2} / (m^*)^{3/2}] G(\Theta), \quad (2)$$

where A includes terms involving the reduced mass of the two ions in the unit cell, the cell volume, the longitudinal-optical frequency, and the effective ionic charge. In the high-concentration range, Moore²² later revised the calculated mobility to take into account the scattering by impurity pairs rather than using the Brooks-Herring²³ (BH) formula which assumes that the impurities scatter the electrons independently. We can simplify the BH formula for ionized-impurity scattering to give the approximate relation between mobility, effective mass, temperature, and impurity concentration N_I :

$$\mu_I \propto [(m^*)^{1/2} / N_I] T^{3/2}. \quad (3)$$

For high-impurity-concentration material, $N_I > 4 \times 10^{17}$ cm⁻³, where the carriers are degenerate and polar scattering is negligible, the approximate mobility relation for degenerate impurity (DI) scattering is discussed by Mansfield.²⁴

Acoustic-phonon scattering, piezoelectric and space-charge scattering will also be present in the Γ_{1C} minimum but to a negligible extent. This conclusion is supported by Connell's²⁵ analysis of the resistivity-pressure relation for Se-doped GaAs to 10 kbar over the concentration range 10^{13} – 10^{19} cm⁻³. He explained his room-temperature results by a dominance of polar scattering for low-concentration samples 10^{13} – 10^{16} cm⁻³, followed by mixed PO and I scattering for $N_I \sim 10^{16}$ – 10^{18} cm⁻³, and finally DI scattering at the highest concentrations.

At high electric fields, several extra scattering effects will take place since electrons can be excited to the satellite minima and to regions of the Γ_{1C} minimum where nonparabolic effects become important. The results of these calculations are

described adequately in the recent high-field review papers.^{26–28} Many of the high-field problems, however, are relevant to the high-pressure results at low electric fields, since under pressure electrons are transferred to the off-center minima. The transfer process from the Γ_{1C} to the X_{1C} minima will take place by LO phonons, provided the three minima are situated at the zone edge. If the minima are situated at Δ_{1C} points, however, then the selection rules are relaxed and transitions involving the LA phonon are also possible.¹⁶ This process is called nonequivalent intervalley scattering, and the mobility can be expressed in a similar form to intravalley acoustic-mode scattering where $\mu_A \propto (m^*)^{-5/2}$.

Intravalley scattering will be unimportant in the Γ_{1C} minimum, but in the high-effective-mass X_{1C} minima it will have more effect. The scattering probabilities between equivalent and nonequivalent valleys depend on the number of valleys involved, their density of states, and the phonon frequency ω_{ij} . Intervalley deformation potential fields D_{ij} are defined to substitute for E_1 , the deformation potential in the acoustic-mode scattering relation, and they give a guide to the strength of scattering between the states. Equivalent intervalley scattering between the X_{1C} minima has been estimated by Hilsun and Welborn⁴ and Fawcett *et al.*²⁸ to be of most importance in limiting the GaAs X_{1C} mobility. Again, the LO phonon will be involved according to the selection rules, and the deformation potential field D_{XX} will be greater than D_{TX} . This is easily seen by noting that the transition rate is proportional to the density of states. Thus, scattering to the low density-of-states Γ_{1C} minimum will be much less probable than to other equivalent X_{1C} states.

The extent of intravalley acoustic-mode scattering in the ellipsoidal X_{1C} minima is difficult to estimate because the relaxation time will be anisotropic, and the deformation potential must be represented by a tensor with components referred to the three perpendicular axes of the ellipsoid. Values for scattering between the X_{1C} minima have been based usually on the comparison with Si,²⁹ i. e., a deformation potential-field value of 1×10^9 eV/cm. The errors could thus be considerable, although James³⁰ has recently estimated a GaAs value close to the Si result. He also obtained 5×10^8 eV/cm for Γ_{1C} - X_{1C} scattering. For a comprehensive review of these deformation potential fields and how they fit the present experimental data, the reader is referred to Fawcett *et al.*²⁸

Experimental and theoretical estimates of the X_{1C} mobility at low fields have given values ranging from 100 to 320 cm²/V sec. Experimental estimates from domain velocities and the fields across the domain would imply a high-field (100 kV/cm) mobil-

ity between 200 and 50 $\text{cm}^2/\text{V sec}$. The wide choice of mobility is probably the result of large variations in the quality of GaAs. The measurements reported in this paper are the first of this type to be made on the high-purity epitaxial material now available.

IV. EXPERIMENTAL

A more detailed account of the experimental apparatus and method has been given previously.³¹ Pressure is applied by opposed tool steel anvils which also act as poles of the magnet giving a field of 6.25 kG at a pole gap of 1.25 mm. The crystal samples were ultrasonically cut in the shape of 2-mm-diameter Van der Pauw cloverleaves, with thicknesses near 0.25 mm. The sample was immersed in epoxy resin at the center of an MgO-loaded epoxy gasket ring. The four copper-wire leads were passed through the gasket.

Standard Hall-voltage and resistivity techniques were employed using a Keithley 150B microvoltmeter. Readings were taken on increasing pressure only, at approximately 3-kbar intervals, and up to five runs were made on crystals cut from each slice. An average pressure variation was

then obtained. Readings on decreasing pressure were not possible since nonhydrostatic stresses are then large and the crystal invariably cracked. Pressure was calibrated using the usual polymorphic transition points of Bi I-II and III-V at 25.4 and 77 kbar, respectively, and Tl I-II at 37 kbar. The pressure repeatability above 25 kbar was ± 1 kbar.

Piezoresistance measurements on $\langle 100 \rangle$ -orientated n -type Si crystals have indicated that the nonhydrostatic stress above 25 kbar is limited to less than 1 kbar using this technique. At lower pressures, the crystal must pass through a compressive nonhydrostatic stress region during gasket formation. The effect of nonhydrostatic stress on the GaAs results is not large in this pressure range, since the electrons still remain in the Γ_{1C} minimum which is isotropic.

A list of the GaAs crystals, over a wide range of doping concentration, is shown in Table I, with the room-temperature and atmospheric pressure electrical parameters. Bulk crystals of good homogeneity (measured as the ratio of resistances at 90° on the cloverleaf) were difficult to obtain at

TABLE I. Characteristics of GaAs samples at atmospheric pressure.

No.	Ingot or slice	$\mu_H[000]$	$(N_D - N_A)$ (cm^{-3})	Resistivity ($\Omega \text{ cm}$)	Thickness (μ)	Doping
Bulk grown						
1	199	4500	1.8×10^{16}	7.62×10^{-2}	250	Se
2	381	4730	5.5×10^{16}	2.48×10^{-2}	250	undoped
3	309(f)	2860	5.5×10^{17}	4×10^{-3}	250	Si
Liquid epitaxy						
4	2LE17	8400	1.49×10^{13}	53.6	160	undoped
5	2LE32	8200	1.65×10^{13}	46.0	75	undoped
6	LE42	8370	3.5×10^{14}	7.0	95	undoped
7	LE15	7150	1.97×10^{15}	4.45×10^{-1}	125	undoped
8	LE11	6900	9.25×10^{15}	9.25×10^{-2}	46	undoped
9	LE149	5650	1.8×10^{16}	6.1×10^{-1}	125	undoped
10	CL9	5450	1.8×10^{16}	6.4×10^{-1}	103	Si
11	LE21	5560	2.36×10^{16}	1.8×10^{-1}	100	undoped
12	CL13	4700	7.3×10^{16}	1.82×10^{-2}	100	Si
13	LE152	3040	6.6×10^{17}	4.6×10^{-3}	150	Se
14	CL17/8	2780	1.54×10^{18}	1.45×10^{-3}	150	Te
15	CL49/19 ^a	2400	1.5×10^{18}	1.7×10^{-3}	50	undoped
16	LE163/41	1850	4.6×10^{18}	7.36×10^{-4}	250	Se
Vapor epitaxy						
17	B123A	8050	6.7×10^{14}	1.15	29	undoped
18	G62A	7350	1.65×10^{15}	5.1×10^{-1}	15	undoped
19	K151A	7300	1.5×10^{15}	5.7×10^{-1}	24	Sn
20	K152A	7000	1.8×10^{15}	4.8×10^{-1}	19.5	Sn
21	K149	6100	1.33×10^{16}	8.0×10^{-2}	12	Sn
22	B73A	6160	2×10^{16}	1.0	10	undoped
23	E76	4000	8.8×10^{16}	1.77×10^{-2}	6	Se
24	E119	3740	1.9×10^{17}	8.66×10^{-3}	5	Se

^aThis sample was grown by a different method. GaAs was added in the form of needles to the gallium. A lower temperature was required before tipping, i. e., 705°C compared with the more normal 800°C. In general, samples produced by this method gave poor surfaces and low mobilities – this was one of the better specimens. The crystal was nominally undoped, but it seems likely that several unidentified impurities were present.

concentrations below 10^{16} cm^{-3} . The mobilities for bulk samples also tended to be lower than for epitaxial material at the same carrier concentration.

The crystal samples were all grown at Standard Telecommunication Laboratories using bulk gradient freeze, liquid and vapor epitaxial techniques. The bulk samples were polished in slices to the required thickness, while the thin layers of epitaxial material were left on $\langle 100 \rangle$ -orientated semi-insulating substrates. Tin contacts were alloyed at 300°C in hydrogen to the degreased crystal surface, and were found to be adequate for the whole concentration range, although extra care in surface preparation had to be taken for carrier concentrations below 10^{15} cm^{-3} to avoid non-Ohmic effects.

V. HALL MEASUREMENT TO 60 KBAR

A resumé of the results is presented in Table II. The resistivity, Hall constant, and mobility are given at 50 kbar together with the measured carrier concentration at atmospheric pressure. Estimates of impurity activation energies relative to the X_{1c} minima are also given.

The results of the crystal measurements could be conveniently divided into three groups: (a) low

carrier concentrations, (b) high carrier concentrations, and (c) samples which could not be fitted to the simple two-band model, applicable to (a) and (b).

A. Low-Impurity-Concentration Material

Material with impurity concentrations below 10^{16} cm^{-3} , where Fermi statistics are not required for the interband transfer calculations, are considered here. As expected, the majority of these purer samples showed little "trapping out" to X_{1c} impurity levels. We discuss specifically samples LE 11 and G 62A; the former showed little or no trapping out and was grown by liquid epitaxy, while the latter exhibited some carrier loss at high pressures and was grown by vapor epitaxy. The other samples in this concentration range could be analyzed in a similar fashion.

The normalized resistivity ρ/ρ_0 , Hall constant R_H/R_{H0} , and Hall mobility μ_H/μ_{H0} curves for LE 11 and G 62A are shown in Figs. 1 and 2. The characteristic resistivity variation for GaAs is found, viz., a slow increase up to 25 kbar followed by a rapid rise to a final saturation at 40 kbar. We can explain this in terms of the band movements

TABLE II. Summary of high-pressure results.

Sample No.	Hall mobility at 50 kbar	$\frac{\mu_H[000]}{\mu_H\langle 100 \rangle}$	$\frac{R_H}{R_{H0}}$	$\frac{\rho}{\rho_0}$	Impurity level activation energy (eV)	
1	120	37.5	2.0	80	0.127	Se
2	300	18.9	2.5	39.5	0.114	undoped
3	100	28.6	1.5	48	0.03	Si
4	340	26.2	1.0	26.2		undoped
	110	76.0	15	1150	large variation about 0.2 eV	
					0.2 eV	
5	390	21.0	0.9	19.0	...	undoped
6	370	23.0	0.9	20.1	...	undoped
7	390	18.3	0.87	16	...	undoped
8	350	19.7	0.89	18.1	...	undoped
9	365	15.5	1.0	15.5	...	undoped
10	390	16.1	1.1	15	0.074	Si
11	350	17.0	1.1	15.5	0.069	undoped
12	370	14.7	1.20	14	0.05	Si
13	230	13.2	1.60	21	0.035	Se
14	220	10.3	1.45	17.5	0.03	Te
15	120	20.0	10.2	260	0.13	undoped
16	110	19.5	1.05	20.5	< 0.01	Se
17	410	19.6	0.9	17.6	...	undoped
18	330	22.3	1.21	27.0	0.15	undoped
19	370	19.8	1.05	18.9	0.065	Sn
20	305	23.05	1.02	22.6	0.048	Sn
21	377	16.2	1.15	18.6	0.040	Sn
22	370	16.6	1.15	19.0	0.081	undoped
23	285	14.0	1.1	14.0	0.03	Se
24	275	13.4	1.25	17.0	0.04	Se

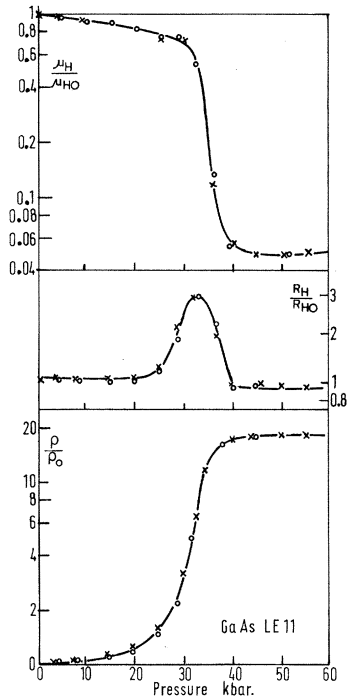


FIG. 1. LE 11. Normalized resistivity ρ/ρ_0 , Hall constant R_H/R_{H0} , and Hall mobility μ_H/μ_{H0} for *n*-type GaAs to 60 kbar at 296 °K; $N_D - N_A = 9.25 \times 10^{15} \text{ cm}^{-3}$, $\rho_0 = 0.92 \text{ } \Omega \text{ cm}$, $\mu_{H0} = 6900 \text{ cm}^2/\text{Vsec}$, liquid-epitaxy layer thickness $46 \text{ } \mu$. Mobility at 50 kbar, $\mu_H(50) = 350 \pm 40 \text{ cm}^2/\text{V sec}$.

with pressure. To 25 kbar, few electrons at low electric fields transfer to the X_{1C} minima, and the small resistivity increase may be ascribed to an increase in effective mass. This effect has been described in detail by De Meis⁹ and by Connell.²⁵ The latter obtained a resistivity increase of 8% at 10 kbar, implying an effective mass-pressure coefficient for the Γ_{1C} minimum of

$$\frac{\partial m_{\Gamma}^*}{\partial P} = (6.0 \pm 0.2) \times 10^{-6} m^*/\text{bar}.$$

Our results for LE 11 and G 62A gave a resistivity increase of 9% to 10 kbar, which is in good agreement with the hydrostatic measurements, considering the nonhydrostatic stresses present in the vicinity of the crystal and difficulties in pressure calibration in this pressure range. Connell²⁵ found that this variation in effective mass of the electrons in the Γ_{1C} minimum could be described by the $\vec{k} \cdot \vec{p}$ perturbation theory provided the increase in direct energy gap was

$$\frac{\partial E_g}{\partial P} = (10.7 \pm 0.5) \times 10^{-6} \text{ eV}/\text{bar}.$$

Above 25 kbar, electrons transfer rapidly to the X_{1C} states with a rapid rise in resistance. At 40 kbar, the full transfer is almost complete and the resistivity curves then level off. By 50 kbar, a

slight decrease is apparent. The resistivity ratios were 18.1 ± 0.9 and 27.0 ± 1.0 for LE 11 and G 62A, respectively.

The Hall-constant pressure curve shows a characteristic maximum near 33 kbar. This type of variation has also been observed during the transfer of electrons to impurity-band conduction in Ge at low temperatures. If the mobility of the final state is much less than that of the initial state, then the maximum in R_H occurs when the conductivities in the two bands are equal from the two-carrier equation, i. e.,

$$n_{\Gamma} e \mu_{\Gamma} \approx n_x e \mu_x. \quad (4)$$

The mobility variations, calculated from R_H/ρ , level off at 50 kbar to give values of 350 ± 40 (LE 11) and $330 \pm 40 \text{ cm}^2/\text{V sec}$ (G 62A), while R_H returns to just below the normalized value for LE 11 and above for G 62A. For the latter sample, this is taken as direct evidence of carrier freeze out of 18% of the carriers to deep impurity levels associated with the X_{1C} minima.

B. Analysis

The expression for resistivity in a two-carrier regime is

$$\frac{\rho}{\rho_0} = \frac{[\mu_{\Gamma}(0)/\mu_{\Gamma}] (N_x/N_{\Gamma}) e^{-(E_x - E_{\Gamma})/kT} + \mu_{\Gamma}(0)/\mu_{\Gamma}}{1 + (\mu_x/\mu_{\Gamma}) (N_x/N_{\Gamma}) e^{-(E_x - E_{\Gamma})/kT}}, \quad (5)$$

where it is assumed that the scattering constant τ is the same for both carriers. This approximation is reasonable near band crossover where a range of scattering mechanisms is present, but

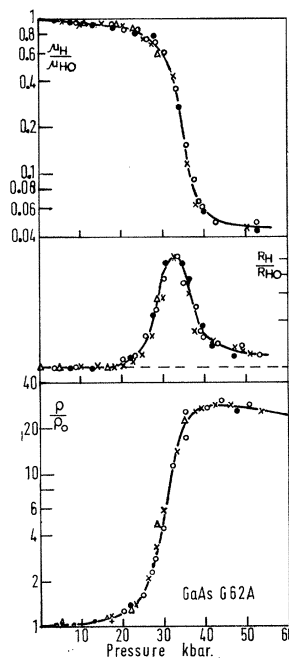


FIG. 2. G 62A. Normalized resistivity ρ/ρ_0 , Hall constant R_H/R_{H0} , and Hall mobility μ_H/μ_{H0} for *n*-type GaAs to 60 kbar at 296 °K; $N_D - N_A = 165 \times 10^{15} \text{ cm}^{-3}$, $\rho_0 = 0.519 \text{ } \Omega \text{ cm}$, $\mu_{H0} = 7350 \text{ cm}^2/\text{V sec}$, vapor-epitaxy layer thickness $15 \text{ } \mu$. Mobility at 50 kbar, $\mu_H(50) = 330 \pm 40 \text{ cm}^2/\text{V sec}$.

account of the changes in ν must be taken when the bands are apart (see Appendix). In Eq. (5) N_i and μ_i are the density of states and Hall mobility, respectively, (i refers to the Γ_{1C} and X_{1C} minima). $E_x - E_\Gamma$ is the subband-gap energy between the Γ_{1C} and X_{1C} states. The values of μ_x and N_x are assumed to be independent of pressure. Slow variations only have been observed in μ_x measured on several samples to 70 kbar; these amount to a slight increase of $\sim 2\%$ per 10 kbar.

For a full analysis, we must consider all the carriers involved and they must obey the equation for charge balance, i. e.,

$$N_D - N_A = n_\Gamma + n_x + n_d, \quad (6)$$

where N_D and N_A are the total number of donor and acceptor electrons, respectively, n_Γ and n_x are the number of electrons in the Γ_{1C} and X_{1C} minima, while n_d is the number of electrons on donor sites. We take $N_D - N_A$ at atmospheric pressure to be the carrier concentration measured by the Hall effect.

For low-concentration material, i. e., $N_D - N_A < 10^{16} \text{ cm}^{-3}$, where the Fermi level is well below E_Γ , to a good approximation, we find

$$n_\Gamma/n_x = (N_\Gamma/N_x) \exp[(E_x - E_\Gamma)/kT]. \quad (7)$$

For the higher concentrations, this approximation breaks down, and the full expression including the Fermi-Dirac integral was used.

For the number of electrons on donor sites,

$$n_d = N_D \left[1 + \frac{1}{g} \exp\left(\frac{\epsilon_x - E_F}{kT}\right) \right], \quad (8)$$

where ϵ_x is the energy of the X_{1C} impurity level and g is the level degeneracy including a spin degeneracy of 2. For uncompensated samples, it is assumed that $N_D \gg N_A$ and so we have used $N_D \approx N_D - N_A$. For compensated samples this approximation is not valid, and the implications are discussed in Sec. VIB.

The conductivity is related to the mobility through

$$\sigma = \frac{n_x e}{\nu} \left(\frac{n_\Gamma}{n_x} \mu_\Gamma + \mu_x \right) = \frac{1}{\rho}. \quad (9)$$

The Hall mobility is given by

$$\mu_H = \frac{\mu_\Gamma [(\mu_x/\mu_\Gamma)^2 + n_\Gamma/n_x]}{(\mu_x/\mu_\Gamma + n_\Gamma/n_x)}. \quad (10)$$

In Eqs. (9) and (10) for the low-concentration material, all the parameters are known with pressure except for n_Γ and n_x . μ_x is taken to be the measured mobility at 50 kbar. The variation of μ_Γ to 50 kbar is taken to be an extrapolation of the linear decrease to 20 kbar. The density of states N_Γ will also increase as the effective mass increases, while N_x is assumed to be constant. This assumption is reasonable considering the small pressure coefficient of the X_{1C} minima and the small pressure

range, i. e., 30–50 kbar, where it becomes effective in the calculations. Both the resistivity and mobility are measured as a function of pressure, and we find that we can fit the data using only two parameters, i. e., $(N_\Gamma/N_x)_{P=0}$ and $(E_x - E_\Gamma)_{P=0}$. However, the pressure coefficients of the two bands must be known. The rate of change of the subenergy gap can be obtained from the resistivity variation since Eq. (5) reduces in the pressure region 20–30 kbar and in the absence of trapping to

$$\ln\left(\frac{\rho(P)}{\rho(0)}\right) - \frac{\mu_\Gamma(0)}{\mu_\Gamma(P)} = \ln\left(\frac{\mu_\Gamma(0) N_x}{\mu_\Gamma(P) N_\Gamma}\right) - \frac{E_x - E_\Gamma}{kT}, \quad (11)$$

i. e., electrons are beginning to transfer to the X_{1C} minima but still contribute little to the mobility since $\mu_x \ll \mu_\Gamma$. A logarithmic plot of

$$\ln\left(\frac{\rho(P)}{\rho(0)}\right) - \frac{\mu_\Gamma(0)}{\mu_\Gamma(P)}$$

against volume for LE 11 using the compressibility data of McSkimin *et al.*³² is shown in Fig. 3, and gives

$$\frac{\partial(E_x - E_\Gamma)}{\partial P} = (1.10 \pm 0.03) \times 10^{-5} \text{ eV/bar}.$$

This is in excellent agreement with previous estimates of 1.08 (see Ref. 15) and $1.15 \times 10^{-5} \text{ eV/bar}$ (see Ref. 8). The intercept at $P = 0$, i. e.,

$$(N_x/N_\Gamma) \exp[(E_x - E_\Gamma)/kT],$$

gives a value for N_x/N_Γ of ~ 50 , for $E_x - E_\Gamma$ at 0.38 eV. Owing to the large extrapolation involved, how-

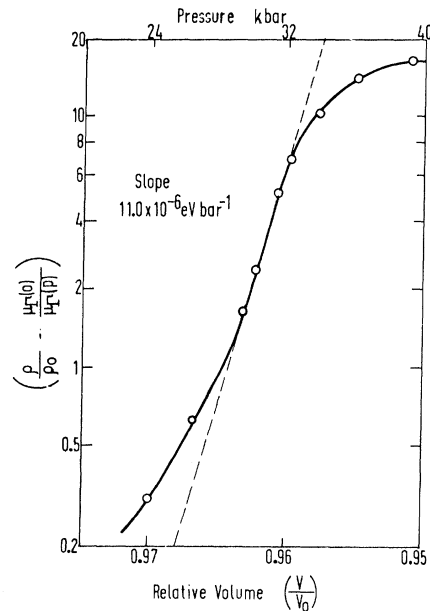


FIG. 3. GaAs LE 11 plot of $[\rho/\rho_0 - \mu_\Gamma(0)/\mu_\Gamma(P)]$ as a function of volume and pressure.

ever, considerable uncertainty must be attached to this result. A subband pressure coefficient of $+1.10 \times 10^{-5}$ eV/bar would agree with the approximate picture of the Γ_{1C} minimum moving at $+1.05 \times 10^{-6}$ eV/bar, and the X_{1C} minima at -0.5×10^{-6} eV/bar.

For sample G 62A, we must take account of the small loss of carriers to donor levels, and Eq. (6) must be satisfied for values of n_d at pressure. It is found that the same paired values of $(N_x/N_\Gamma)_{P=0}$ and $(E_x - E_\Gamma)_{P=0}$ fit both LE 11 and G 62A with an X_{1C} impurity level 0.15 ± 0.04 eV below E_x for G 62A, giving the mobility plots shown in Fig. 4. Credible values of n_Γ and n_x which fit G 62A are shown in Fig. 5 using these parameters; note that by 50 kbar, $n_x < n_\Gamma$ and carriers have been lost to the donor-impurity level.

Figure 4 shows the agreement between theoretical and experimental mobilities for all the low-concentration material. The paired parameters which fit the data are shown in Fig. 6. We see that a subband gap of 0.38 eV requires a density-of-states ratio $(N_x/N_\Gamma)_{P=0}$ of 45. If the Γ_{1C} density-of-states effective mass m_Γ^* is taken as $0.065m_e$, then the X_{1C} density-of-states effective mass will be $0.82m_e$. For three minima, the effective mass in

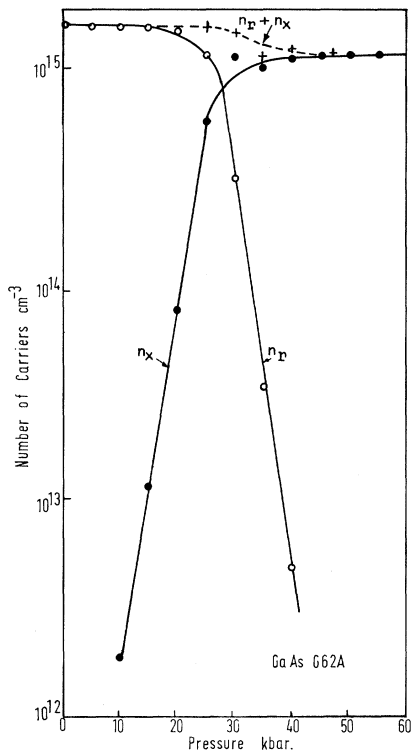


FIG. 4. Theoretical fits of mobility pressure results for GaAs samples LE 11 and G 62A to a simple two-band model.

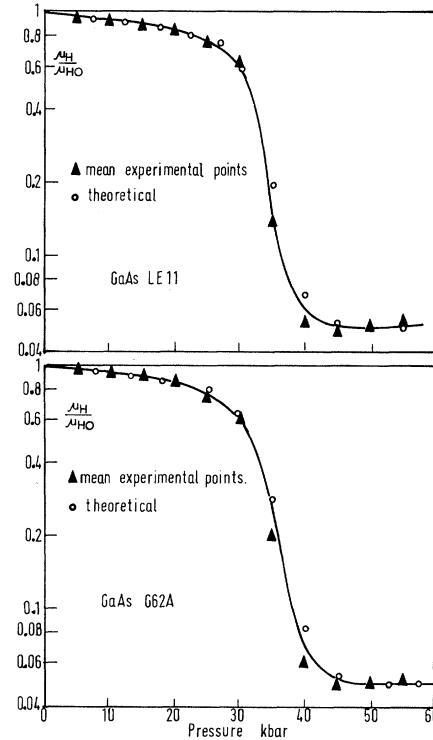


FIG. 5. Plots of n_Γ and n_x versus pressure for GaAs G 62A. At 50 kbar, $n_x < n_\Gamma$ inferring carriers have been lost to an impurity level or levels associated with X_{1C} minima.

one minimum is then $0.394m_e$. For $m_\Gamma^* = 0.067m_e$, $m_x^* = 0.85m_e$ and the effective mass in one minimum is $0.41m_e$. A subband gap of 0.38 eV is determined from the maximum in R_H/R_{H0} which occurs approximately 1.5 kbar before band crossover. From consideration of Eq. (4), this was observed at a mean pressure of 33 ± 1 kbar for the purer samples which exhibited negligible carrier trap out. An energy gap of 0.38 ± 0.01 eV then follows from the subband pressure coefficient of 11×10^{-6} eV/bar.

C. High Carrier Concentration

The GaAs samples studied in the concentration range 10^{17} – 10^{19} cm^{-3} were grown by bulk- and liquid-epitaxy techniques for use as laser material. Considerable variation in results was found for these samples and this is shown in Figs. 7–9 which give the resistivity, Hall constant, and X_{1C} mobility curves for three samples. Samples CL 17/8 (14) and CL 49/19 (15) (the numbers in parentheses refer to Fig. 10 and Table I), although having nominally the same dopant and carrier concentration, lost carriers in wildly differing amounts at high pressures.

In the low-pressure region, most samples exhibited no carrier loss to 15 kbar. The resistance in-

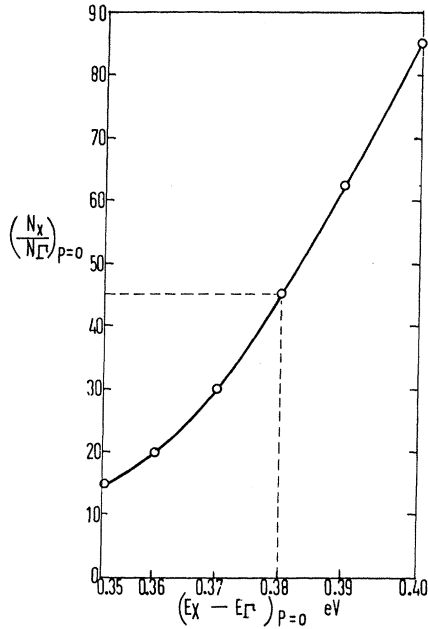


FIG. 6. Paired parameters of $(N_x/N_T)_{P=0}$ and $(E_x - E_T)_{P=0}$ which fit the simple two-band model for high-purity GaAs.

crease was thus assumed to be a mobility change. This allowed Connell²⁵ to make his analysis of the resistivity variation in GaAs below 10 kbar under hydrostatic conditions, and our results are in excellent agreement in the high-concentration range. The larger resistivity change with pressure, e.g., $\rho(10)/\rho(0) = 1.22$ for $n \sim 1.5 \times 10^{18} \text{ cm}^{-3}$, can be explained qualitatively by the increase in importance of ionized-impurity scattering and the degenerate-impurity scattering described by Mansfield.²⁴ The more recent quantum transport theory of Moore²² would probably give a more accurate analysis of the situation in this concentration range, but the analysis leads to large computational difficulties and for our treatment Connell's²⁴ simple analysis is quite adequate.

Extrapolation of the linear resistivity variation to 10 kbar can only be an approximation for high impurity concentrations. The extent of nonlinearity will depend on the dominance of the different scattering mechanisms. If, as seems likely, degenerate-impurity scattering predominates, i. e., $\mu \propto (m^*)^2$, then in the degenerate region the resistivity equation

$$\frac{\rho(10)}{\rho(0)} = \left(\frac{m_F^*(10) \chi_s(0)}{m_F^*(0) \chi_s(10)} \right)^2 \times \left[1 + \left(\frac{m_F^*(0)}{m_F^*(10)} \right)^{3/2} \frac{N_x}{N_T} \exp \left(- \frac{(E_x - E_T)_{P=10}}{kT} \right) \right] \quad (12)$$

can be simplified, in terms of the mobility for negligible carrier loss to the X_{1C} minima, to

$$\frac{\mu_T(0)}{\mu_T(10)} = \left(\frac{m_F^*(10) \chi_s(0)}{m_F^*(0) \chi_s(10)} \right)^2 = \frac{m_F^*(10)}{m_F^*(0)} (1.03)^2, \quad (13)$$

where the pressure variation of χ_s , the dielectric constant, is taken from De Meis.⁹ The calculated Γ_{1C} mobility from Eq. (14) does not begin to deviate significantly from the linear extrapolation until after 30 kbar, when the importance of such a discrepancy becomes negligible anyway, owing to the dominance of the low-mobility X_{1C} electrons.

The onset of carrier transfer to the χ_{1C} minima will occur at lower pressures than for the purer material, since the Fermi level is now above the bottom of the Γ_{1C} minimum. Hence, the resistivity and R_H curves reach a maximum at slightly lower pressures.

Theoretical and experimental mobilities for CL 17/8 (14), CL 49/17 (15), and 309 (F) (3) are shown in Fig. 9. The same paired values of $(N_x/N_T)_{P=0}$ and $(E_x - E_T)_{P=0}$ were used as for the low-concentration material. A small increase in the effective mass of the Γ_{1C} electrons would be expected, due to nonparabolicity, but the effect will be small¹⁰ (<5%) even at a concentration of $1.5 \times 10^{18} \text{ cm}^{-3}$ and should have little effect on the validity of the calculations.

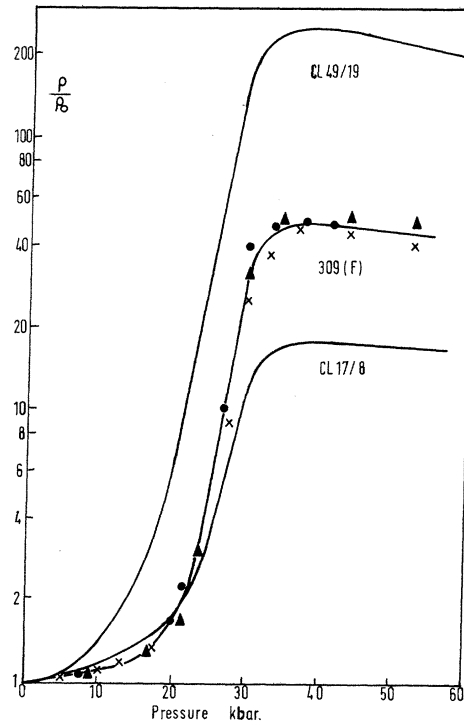


FIG. 7. Normalized resistivity ρ/ρ_0 for high-impurity-concentration n -type GaAs to 60 kbar at 296°K. CL 17/8 and CL 49/19, liquid epitaxy, $N_D - N_A = 1.5 \times 10^{18} \text{ cm}^{-3}$; 309(F), bulk grown, $N_D - N_A = 5.5 \times 10^{17} \text{ cm}^{-3}$. The experimental points on 309(F) are shown to illustrate the experimental scatter. The curves for CL 17/8 and CL 49/19 are the mean results.

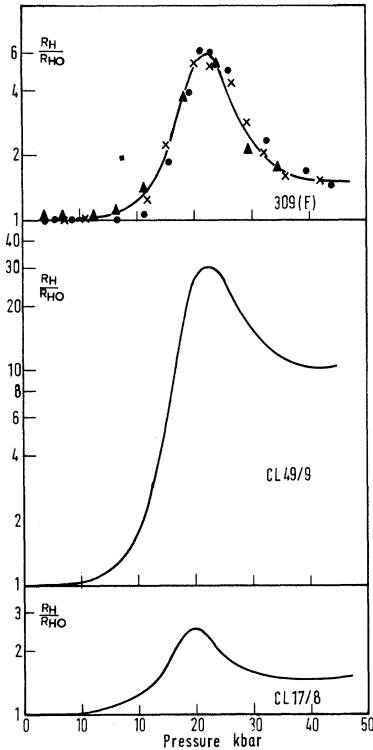


FIG. 8. Normalized Hall constant R_H/R_{H0} for high-impurity-concentration n -type GaAs to 60 kbar at 296 °K. CL 17/8 and CL 49/19, liquid epitaxy, $N_D - N_A = 1.5 \times 10^{18} \text{ cm}^{-3}$; 309(F), bulk grown, $N_D - N_A = 5.5 \times 10^{17} \text{ cm}^{-3}$. The experimental points on 309(F) are shown to illustrate the experimental scatter. The curves for CL 17/8 and CL 49/19 are the mean results.

At very high concentrations (i. e., $> 5 \times 10^{18} \text{ cm}^{-3}$), this will not, of course, be true.

The large scatter of X_{1C} mobilities and the activation energies of impurity levels found in these high-

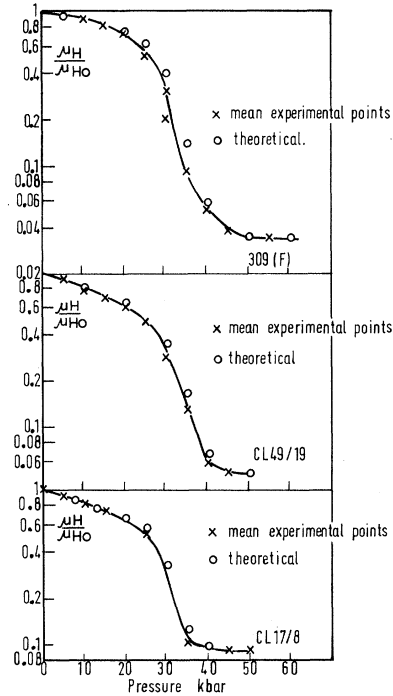


FIG. 9. Normalized Hall mobility μ_H/μ_{H0} for high-impurity-concentration n -type GaAs to 60 kbar at 296 °K. CL 17/8 and CL 49/19, liquid epitaxy, $N_D - N_A = 1.5 \times 10^{17} \text{ cm}^{-3}$. Theoretical fits to the simple two-band model are shown.

concentration samples are discussed in the following sections.

VI. X_{1C} MOBILITY

A. Variation of X_{1C} Mobility with Carrier Concentration

A full plot of the experimental X_{1C} mobilities at 50 kbar and room temperature is shown in Fig. 10 as a function of atmospheric pressure carrier concen-

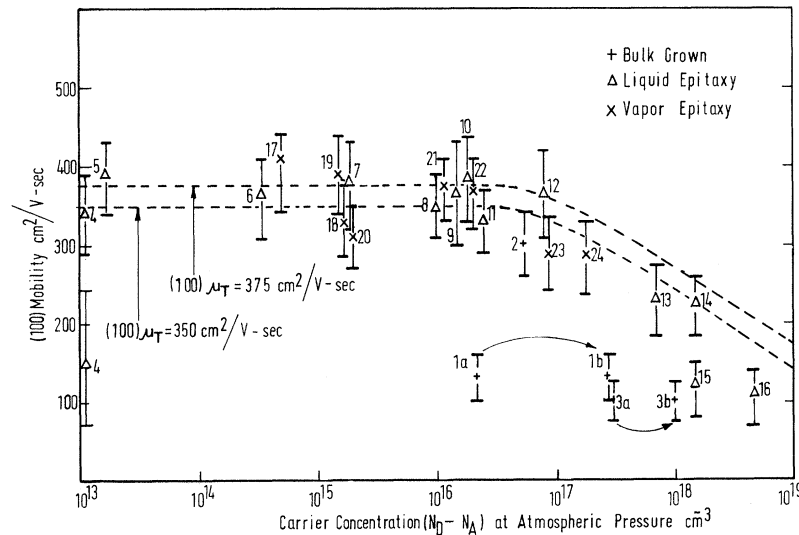


FIG. 10. Plot of GaAs- X_{1C} Hall mobilities at 50 kbar and 296 °K versus impurity concentration, where it is assumed $N_I \approx N_D - N_A$, or $N_D \gg N_A$. The effect that the neglect of compensation might have on this plot is shown by samples 1 and 3 which could be moved to positions 1B and 3B (see text). This approximation probably accounts to a large extent for the large scatter in mobility results near $N_D - N_A \approx 10^{18} \text{ cm}^{-3}$. The key to the plot is given in Table II. The X_{1C} results have been fitted using simple BH impurity scattering with $1/\mu = 1/\mu_T + 1/\mu_I$, where μ_T is taken as 350 and 375 $\text{cm}^2/\text{V sec}$, obtained from the low-concentration material results. Impurity scattering appears to have little effect until $N_D - N_A > 10^{17} \text{ cm}^{-3}$.

tration $N_D - N_A$ over the range 10^{13} – 10^{19} cm^{-3} . Little variation of the mobility was found from 10^{13} to 10^{17} cm^{-3} ; thus, ionized-impurity scattering has a negligible effect for this material. The influence of impurity scattering has been found to be more apparent at lower concentrations in the Γ_{1C} minimum.

The data in Fig. 10 have been fitted very simply by using the addition of reciprocal mobilities $1/\mu = 1/\mu_T + 1/\mu_I$, where μ_T is the experimental mobility for low-carrier-concentration material. Two values are shown at 375 and 350 $\text{cm}^2/\text{V sec}$. μ_I is BH scattering where m_x^* is taken as $0.41m_g$. We find that BH scattering only becomes important towards $N_D - N_A = 10^{18}$ cm^{-3} , and the mobility falls to about 170 $\text{cm}^2/\text{V sec}$ at 10^{19} cm^{-3} . The curves are slightly higher than our experimental results for $N_D - N_A$ greater than 10^{18} cm^{-3} . This is not surprising considering the known inhomogeneity and close compensation of these very high-impurity-concentration samples, which also accounts for the considerable scatter of results found in this region. It is known that precipitates of Ga_2Te_3 ³³ and Ga_2Se_3 ³⁴ form above 10^{18} cm^{-3} . Also, the unknown extent of compensation in these samples could well mean that the total ionized-impurity concentration is much higher than is given by the first approximation of $N_D - N_A$ used here. Some mobility results undoubtedly refer to higher concentrations as far as scattering is concerned. Moreover, BH theory for scattering by impurities assumes that the impurities scatter the electrons independently, and this also is a considerable simplification for these concentrations. Corrections following Moore²² would give a decrease in the mobilities implied by the simple model. Under the circumstances, the fit of the simple model to experiment is reasonable and it clearly shows that ionized-impurity scattering has little effect on the X_{1C} Hall mobility for $N_D < 10^{17}$ cm^{-3} .

The X_{1C} mobilities near $(N_D - N_A)10^{15}$ cm^{-3} at 50 kbar are in the region 350–375 $\text{cm}^2/\text{V sec}$. We have assumed in our analysis in Sec. V that this mobility is constant with pressure in view of the very small increases of mobility with pressure observed in $\langle 100 \rangle$ electrons in Si and GaP. Also, our measurements in GaAs to 70 kbar have confirmed only a very small increase at higher pressures ($\sim 2\%/10$ kbar). Such a change will have a negligible effect in our calculation, since μ_x only becomes important beyond 30 kbar. We estimate the mobility at 50 kbar to be 375 ± 45 $\text{cm}^2/\text{V sec}$, but if we extrapolate to atmospheric pressure, taking account of the small mobility increase with pressure, we have 340 ± 45 $\text{cm}^2/\text{V sec}$. Taking account of the scattering constant r (see Appendix), we obtain a conductivity mobility of 328 ± 50 $\text{cm}^2/\text{V sec}$.³⁵ This result is still higher than previous experimental^{7,8} and theoretical estimates.³⁶ Fawcett *et al.*,²⁸ however, recently estimate an X_{1C} mobility at low fields of 325 cm^2/V

sec. In this calculation, spherical bands are assumed and the mobility is limited by three components, polar-optical (PO), acoustic-mode (DP), and intervalley scattering. The last is the most important and assumes the deformation potential (field) to be the same as in Si, i. e., 1×10^9 eV/cm, and the angular frequency of the LO phonon, $\omega_l = 4.54 \times 10^{13}$ rad/sec. The satisfactory agreement between our experimental value and theory supports their use of this deformation potential.

No significant difference was observed between the mobilities of X_{1C} electrons for samples with different doping, i. e., with Se, Si, Sn, and Te. The same has been observed for Γ_{1C} electrons.

B. Anomalous Results

Several anomalous results were found. Samples 199 (1), 309(F) (3), and 2LE17 (4) exhibited mobilities at high pressures well below those observed by other crystals. (Numbers in parentheses refer to Fig. 10 and Table I.) The first two were bulk grown and gave mobilities of 120 ± 20 and 100 ± 10 $\text{cm}^2/\text{V sec}$, respectively.

The possibility that surface defects resulting from cutting of the ingot, and the ensuing lapping process, might have had some effect was eliminated by carrying out experiments on ingot 199 with different degrees of polished surface. Only a small increase of $\sim 10\%$ in X_{1C} mobility was observed between 200- and 1- μ finishes.

Sample 2LE17 (4) was made by liquid epitaxial techniques and was studied extensively. The slice had a flat shiny surface near the center of about 1-cm diameter, but ripples were apparent away from this region. It is thought that the ripples are evidence of constitutional supercooling. A number of cloverleaf samples were taken over the slice. Results from the center gave the high X_{1C} mobility with negligible carrier loss, while those from the outer region gave varying mobility values ranging from 100 to 120 $\text{cm}^2/\text{V sec}$, with different amounts of trapping out. The homogeneities of these samples, as measured by the resistance ratios at constant current at 90° across the cloverleaf, were poor (ratios from 2 to 4 were obtained). For the better more homogeneous samples, this value was usually less, tending towards unity. Because of the obvious inhomogeneity in 2LE17 (4), these low-mobility X_{1C} results could not be expected to be explained on the present theory.

To explain the extremely low mobilities in some of these bulk samples, we require a scattering mechanism which seems to affect the X_{1C} electrons to a greater extent than the Γ_{1C} electrons, e. g., the Γ_{1C} mobility of 199 (1) is 4500 $\text{cm}^2/\text{V sec}$, compared with 6000 $\text{cm}^2/\text{V sec}$ for an epitaxial sample with similar carrier concentration, yet the X_{1C} mobilities are 150 compared to 350 $\text{cm}^2/\text{V sec}$. The possibili-

ty that an orientated scattering center could be preferentially scattering $\langle 100 \rangle$ electrons is unlikely. Bulk-grown GaAs was grown in silica boats at 100 °C, and SiO_4 tetrahedra could be present in the ingot, but other bulk-grown samples (e.g., 381) gave a high X_{1C} mobility value in agreement with the epitaxial crystals.

The low Γ_{1C} mobilities of some bulk samples and the associated trapping out indicates that in these samples also the anomalous effect is linked with the impurities and inhomogeneity. If we take the mobility as an approximate estimate of impurity concentration, then 199 (1) should have a concentration near $3 \times 10^{17} \text{ cm}^{-3}$ compared with the $N_D - N_A$ value of $2 \times 10^{16} \text{ cm}^{-3}$. Similarly 309 (F) (3) will have $N_I \sim 10^{18} \text{ cm}^{-3}$ compared with $N_D - N_A$ of $3 \times 10^{17} \text{ cm}^{-3}$. Thus, in Fig. 10, we have moved the position of 199 on the carrier-concentration scale from 1A to 1B, and 309(F) from 3A to 3B. The anomaly then becomes less apparent. In Fig. 11, we show the normalized resistivity, Hall constant and mobility for 199 (1). The theoretical mobility fit is calculated in the same way as for the high-concentration material, using the same adjustable band parameters. The fit is poor compared with the other samples. Figure 12 is a plot of the values of n_T and n_x with pressure for 199 (1), again showing carrier loss to an X_{1C} impurity level.

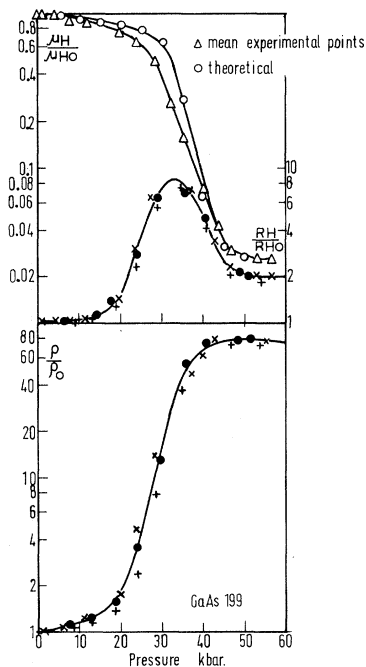


FIG. 11. Ingot 199. Normalized resistivity ρ/ρ_0 , Hall constant R_H/R_{H0} , and Hall mobility μ_H/μ_{H0} for n -type GaAs to 60 kbar at 296 °K; $N_D - N_A = 1.8 \times 10^{16} \text{ cm}^{-3}$, $\rho_0 = 7.62 \times 10^{-2} \Omega \text{ cm}$, $\mu_{H0} = 4500 \text{ cm}^2/\text{V sec}$, bulk grown. Mobility at 50 kbar = $120 \pm 20 \text{ cm}^2/\text{V sec}$.

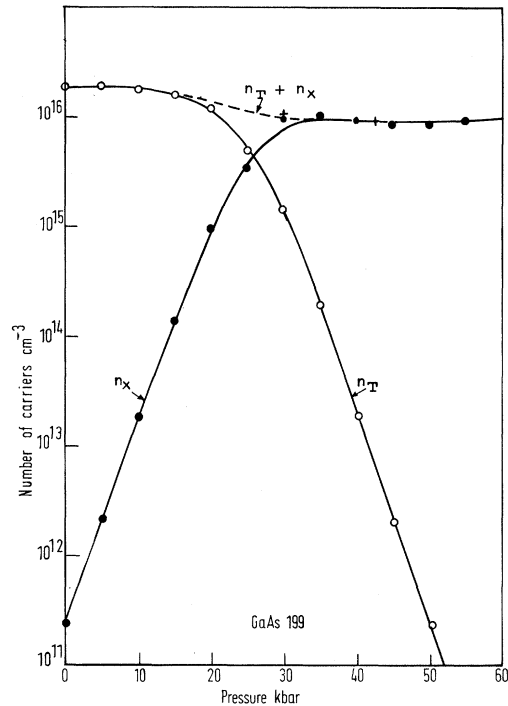


FIG. 12. Plots of n_T and n_x for GaAs 199. At 50 kbar, $n_x < n_T$, implying that carriers have been lost to an impurity level or levels associated with the X_{1C} minima.

We suggest therefore that the anomalously low mobilities occur in highly compensated inhomogeneous samples. The 10^{13} cm^{-3} epitaxial sample 2LE17 (4) was obviously of this category, and for cloverleaves taken from the outer regions of the slice there may even be p -type regions in the matrix. Certainly, Schottky diode carrier-concentration profiles with depth on similar slices of material to this (i.e., 10^{13} cm^{-3}) have produced changes of an order of magnitude in $N_D - N_A$ within a few μ vertically and perhaps a factor of 4 laterally.³⁷ [Later material of which 2LE32 (5) is a typical example show more constant lateral and vertical concentration profiles.] At high pressures when electrons are lost to the X_{1C} impurity levels, the cross section of these inhomogeneous charge regions could increase. Weisberg³⁸ has used a similar effect to explain anomalously low Γ_{1C} mobilities. According to Gossick,³⁹ the effective cross section of the space-charge region will also increase for low carrier concentrations.

Hall-effect measurements on such material must therefore be considered with caution, since only an averaged conductivity through the layer is observed. Recent low-temperature measurements on this low-carrier-concentration material have shown that a sample with a low room-temperature mobility can have a relatively high peak mobility at 77 °K compared with a sample which has a high Γ_{1C} mobility

near $8000 \text{ cm}^2/\text{V sec}$ at 296°K . This can be seen by comparing measurements³⁷ on two samples, e.g., 1LE4,

$$N_D - N_A = 1 \times 10^{12} \text{ cm}^{-3}, \mu_H (296^\circ\text{K}) = 4500 \text{ cm}^2/\text{V sec}$$

and

$$\mu_H (77^\circ\text{K}) = 80\,000 \text{ cm}^2/\text{V sec},$$

while 2LE17,

$$N_D - N_A = 1.5 \times 10^{13} \text{ cm}^{-3}, \mu_H (296^\circ\text{K}) = 7800 \text{ cm}^2/\text{V sec}$$

gave

$$\mu_H (77^\circ\text{K}) = 84\,000 \text{ cm}^2/\text{V sec}.$$

This effect is probably analogous to the high-pressure results where in both cases the current paths through the crystal are changing under different ambient conditions as regions of inhomogeneity alter shape. This is also supported by the homogeneity factor which changed by a factor of 2 during high-pressure experiments on the poorer-quality 2LE17 (4) samples.

Typical low-temperature Hall data for the low-concentration liquid-epitaxial material grown at STL are given in the recent results of Hicks and Manley,⁴⁰ and Chamberlain and Stradling.¹¹ One of our samples, 2LE32 (5) is plotted in the first paper.

VII. X_{1C} IMPURITY LEVELS

The trapping out of carriers during the transfer process to levels associated with the X_{1C} minima has been directly observed. The properties of impurity levels associated with higher-lying minima have been discussed using previous experimental results by Paul.⁴¹ For a more theoretical discussion of the problem, the reader is referred to the review by Kosicki.²⁰ The extent of carrier loss to these levels at high pressures has to date been inferred from simple resistivity measurements, but the Hall measurements have shown for certain that carriers can be frozen out. Ideally, low-temperature measurements at high pressures are required to obtain accurate impurity energies, but estimates can be made from the present results. The Hall and resistivity data have been fitted in those samples where carrier loss occurred by including the term n_b , given by Eq. (8). The activation energy of the level can be determined by substituting different values of the Fermi level and ϵ_x in the charge-balance equation (7). The assumption that N_D is approximately equal to $N_D - N_A$, however, will not apply for highly compensated samples, and as we have seen, this may account for some of the mobility misfit found in ingot 199 (Fig. 12). Furthermore, this method is highly insensitive for an accurate determination of the level for low-concentration material owing to the large energy difference between E_F and E_x . Thus, taking LE 11 as an ex-

ample, it is possible to insert a level below E_x and still obtain a reasonable fit to the results for any $E_x - \epsilon_x < 0.06 \text{ eV}$. For higher donor concentrations, however, where the Fermi level is closer to E_x , we can obtain reasonably accurate estimates for ϵ_x .

Figure 13 is a plot of the activation energies derived for a number of samples against $N_D^{1/3}$ in cm^{-1} . There is a tendency towards higher activation energies at lower concentrations in agreement with Pearson and Bardeen,⁴² who found that the binding energy decreases with increasing donor or acceptor concentration. Montgomery⁴³ obtained a similar variation for Te-doped GaP. There is a considerable scatter in our results, but it appears to separate out into two groups near 0.045 and 0.14 eV. At concentrations between 10^{17} and 10^{18} cm^{-3} , we see no apparent difference between the lower activation energies of Si, Se, and Te near 0.045 eV. This result is in reasonable agreement with the work of Craford *et al.*⁴⁴ who studied GaAs/P alloys to high pressure and found an activation energy of 0.03 eV for Te-doped material with carrier concentrations near 10^{18} cm^{-3} . Holonyak *et al.*⁴⁵ found that for these alloys the S level was deeper than for Te. This effect has also been seen in GaSb where Kosicki *et al.*⁴⁶ interpret the resistivity data for transfer to the X_{1C} minima in S, Se, and Te material in terms of deep levels, with the sulphur excitation energy at 0.32 eV and the Se and Te levels at lower energies. These are very deep levels, however, and cannot be considered in terms of the hydrogenic model. The variation of resistivity obtained by Pitt²¹ for Te-doped GaSb was very similar to that obtained by Kosicki *et al.*⁴⁶ for Se doping, so the possibility that these deep levels are caused by a complex or common crystal defect must not be ig-

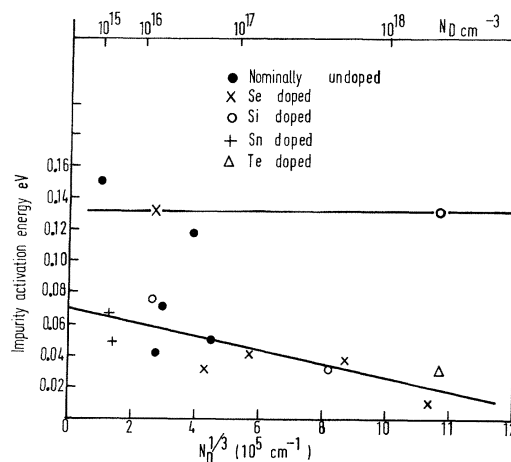


FIG. 13. Plot of activation energy for impurity levels of Si, Se, Te, and Sn relative to the X_{1C} minima versus $N_D^{1/3} \text{ cm}^{-1}$ (i.e., as a function of mean interimpurity distance).

nored. The deep GaAs impurity levels near 0.14 eV are apparently constant with impurity concentration. We note that for samples with deep levels in GaAs, e.g., G 62A, at pressures extending above 50 kbar the number of carriers increased slowly accompanied by a drop in resistivity. This did not occur in samples with shallow donors, e.g., LE11. The two results may be compared in Figs. 1 and 2 and would be expected if the deep levels move with smaller pressure coefficients than the X_{1C} . On the other hand, shallow donors would be expected to move more closely with the band edge and thus produce only a slight change in the number of carriers. In our calculations, we have assumed there is only one level, but it is probable that several are present. The results will tend to be dominated by the deeper level, and complications will arise if other shallower levels are occupied. Such calculations contain too many unknowns, and so the deeper activation energies must be accepted with this further reservation. Finally, we note that Hutson *et al.*⁷ have obtained a still deeper X_{1C} level due to S in GaAs near 0.2 eV from a low-temperature experiment at high pressures.

We are able to compare our results for the shallow donors in the high-impurity-concentration range directly with measurements made on excitation energies in GaP. Montgomery⁴³ obtained a level 0.07 ± 0.01 eV below E_x for Te-doped GaP. If we assume the hydrogenic model where $\epsilon_1 \propto m^*/x_s^2$, we obtain an approximate activation energy of 0.05 eV taking the static dielectric constants as 11.1 (GaP) and 12.5 (GaAs) and the effective masses as $0.35m_e$ and $0.41m_e$, respectively. (The GaAs dielectric constant is assumed constant with pressure to a first approximation.) This is slightly higher than our experimental result of 0.045 ± 0.01 eV, but agrees within experimental error.

Comparison with GaAs Γ_{1C} excitation energies also gives an X_{1C} level at 0.036 eV, taking the Γ_{1C} excitation energies near 0.006 eV found by Summers *et al.*⁴⁷ from infrared photoconductivity measurements, and $m_{\ddagger}^* = 0.065m_e$. This is in good agreement with our results, and we conclude that to a first approximation the hydrogenic model gives reasonable estimates for shallow X_{1C} activation energies in GaAs.

VIII. CONCLUSIONS

The X_{1C} mobility in GaAs has been determined at 375 ± 40 cm²/V sec at 50 kbar. Extrapolating to atmospheric pressure, we expect a value of 328 ± 50 cm²/V sec. On the basis of this result and comparing with the theoretical calculations of Fawcett *et al.*,²⁸ we find that the intervalley-scattering deformation potential field D_{xx} should be close to the 1×10^9 eV/cm found for Si.

Our Hall measurements can be fitted using a very

simple two-band model where

$$(a) \quad \frac{\partial(E_x - E_{\Gamma})}{\partial P} = (11.0 \pm 0.3) \times 10^{-6} \text{ eV/bar},$$

$$(b) \quad (N_x/N_{\Gamma})_{P=0} = 45_{-9}^{+11},$$

and

$$(c) \quad (E_x - E_{\Gamma})_{P=0} = 0.38 \pm 0.01 \text{ eV}.$$

We can now make certain deductions concerning the band structure. Recent theoretical calculations in III-V compounds indicate that GaP and GaSb have six $\langle 100 \rangle$ minima situated at Δ points in from the zone edge, while GaAs could have only three. Experimental results on GaP seem to support the six-minima hypothesis, while the evidence for GaSb and GaAs is still doubtful. Gaylord and Rabson⁴⁸ find that for GaAs, taking Ehrenreich's¹³ density-of-states effective mass of $1.2m_e$, and taking $m_l = 1.3m_e$ ³³ and $m_t = 0.23m_e$,¹⁸ the number of minima given by

$$\nu_x = [m_x^*/(m_l m_t^2)^{1/3}]^{3/2}$$

will be six. Assuming $m_{\ddagger}^* = 0.065m_e$, our density-of-states effective mass m_x^* is $0.82m_e$. If we take the above theoretical values for m_l and m_t , we find $\nu_x = 2.83$ and m_x^* (one minimum) = $0.394m_e$. For $m_{\ddagger}^* = 0.067m_e$, then $m_x^* = 0.85$, $\nu_x = 2.98$, and m_x^* (one minimum) = $0.41m_e$. Since ν_x cannot be less than 3, our result supports the theoretical prediction that there are only three minima and that they are situated at the zone edge. In this case, the intervalley-scattering rules can be resolved and intervalley scattering will be by LO phonons only. The possibility that the effective number of minima could vary between three and six depending on the exact position of the minima relative to the zone edge is intriguing. The effective number will depend on temperature, and it should not be unrealistic to say we obtain three minima at room temperature. The low mobilities obtained in the $\langle 100 \rangle$ minima in GaP and GaSb to date could partly result from the added scattering caused by the presence of six minima. Close investigation of GaAs/P alloys might reveal interesting effects with temperature with the possibility of changeover from three to six minima.

These high-pressure results will not necessarily give an accurate reflection of high-field Gunn conditions. The difficulty lies with the position of the four L_{1C} minima relative to the X_{1C} minima. At high pressures, these will move away from the valence and X_{1C} bands, and the low-field electrons at high pressures will only "see" the X_{1C} minima, whereas at high fields and atmospheric pressure, the electrons could be excited to both sets of minima. Thus, the total high-energy density of states will be greater than our value of $0.85m_e$, and the theoretical effective mass which is usually taken as $1.2m_e$ in high-field calculations could possibly be

near the correct value. This will depend on the effective masses in the ellipsoidal L_{1C} minima. The L_{1C} density-of-states effective mass for GaSb, for example, has been measured between 0.43 and $0.53m_e$ ^{49,50} and for Ge it is $0.56m_e$.⁵¹ The mobility of L_{1C} electrons is greater than X_{1C} electrons again by analogy with GaSb, but the proximity of the L_{1C} and X_{1C} minima will add to the possible nonequivalent scattering. For accurate calculation, this means that further deformation potentials are required to account for $\Gamma_{1C}-L_{1C}$, $X_{1C}-\Gamma_{1C}$, and $L_{1C}-L_{1C}$ scattering. The high-field calculations will then be extremely complex, and so knowledge of the location and effective masses of the L_{1C} minima is thus of great importance. It is difficult at present to see how this mass can be measured, apart from uniaxial stress experiments. If Jones and Lettington⁵² are correct and the L_{1C} minima are 0.4 eV above the X_{1C} minima, this problem is small; however, the measurements of James *et al.*¹⁷ indicate that they are only 0.09 ± 0.01 eV above the X_{1C} minima at atmospheric pressure.

Our experiments over a wide impurity concentration have shown that ionized-impurity scattering is unimportant below 10^{17} cm⁻³ in the X_{1C} minima. This result can now be used with confidence on Gunn material which is typically in the region 10^{14} - 10^{16} cm⁻³. Anomalous results which gave low mobilities near 150 cm²/V sec can be explained in terms of high compensation and inhomogeneity. At high concentrations, $>10^{18}$ cm⁻³, where the inhomogeneity became greater owing to precipitates of compounds, e.g., Ga₂Te₃ for Te-doped material, the X_{1C} mobilities are scattered over a wide range.

The presence of impurity levels associated with the higher-lying X_{1C} minima have been directly observed and compared with the hydrogenic model. For shallow impurities, near 0.045 ± 0.01 eV below the X_{1C} minima for Se, Si, Te at $N_D - N_A \sim 10^{17}$ cm⁻³, the model is found to be a reasonable approximation. It is suggested that deeper levels observed in some samples near 0.14 eV could be due to a complex or structural defect. The pressure coefficients of the deeper levels tend to be less than those of the associated X_{1C} minima. Little theoretical and experimental work has been reported on the implications of such higher-lying impurity levels for high-electric-field carrier-transfer effects. Typically, we would expect the shallow Si, Se, Te, and Sn levels (from Fig. 13) to have an activation energy near 0.06-0.08 eV for Gunn-effect material in the carrier-concentration range 10^{15} - 10^{16} cm⁻³.

ACKNOWLEDGMENTS

The study was financed by a Ministry of Technology contract, and crystals were grown at S. T. L. by D. E. Bolger, A. R. Goodwin, H. G. B. Hicks, and A. Kaiser. The authors are grateful to these,

and to Professor P. N. Butcher, Dr. W. Fawcett, Professor C. H. L. Goodman, D. F. Manley, Dr. H. D. Rees, and Dr. R. A. Stradling for helpful discussions.

APPENDIX

For a number of samples, R_H dropped below its original normalized value by 50 kbar (see Table II). We explain this in terms of changes in the scattering factor r , where $R_H = -r/ne$ or $r = \mu_H/\mu_C$ and μ_C is the conductivity mobility.

The scattering factor is normally defined as the ratio of relaxation-time averages, i. e.,

$$r = \langle \tau^2 \rangle / \langle \tau \rangle^2,$$

and under low-magnetic-field conditions, $r = 1.18$ for acoustic-mode lattice scattering and 1.93 for pure ionized-impurity scattering. For PO scattering, however, τ is not a simple function of energy (e.g., $\tau = E^3$) and cannot be defined, except in the limit of very high temperatures. r will thus depend on Θ/T , where Θ is the characteristic temperature of the lattice associated with the optical-frequency mode ν_1 by $k\Theta = h\nu_1$, and for $T \gg \Theta$, the relaxation time τ varies as $E^{1/2}$. The method of solving the Boltzmann transport equation (to obtain results at lower temperatures) using a variational formulation has been discussed in detail by Howarth and Sondheimer.⁵³ The solutions in low magnetic fields have since been determined for the Hall and magnetoresistance coefficients by a number of workers. At high magnetic induction, when μB in practical units exceeds 10^8 , $r \rightarrow 1.0$. Thus, we are working in the low-field region for the Γ_{1C} minimum in GaAs for typical mobilities of 6×10^3 cm²/V sec and magnetic field of 6.25×10^3 G. This has been found to be experimentally correct by Wolfe *et al.*⁵⁴ who measured the mobility at high and low fields for similar high-mobility GaAs at room temperature. In our experiments, electrons in the low-mobility X_{1C} minima must certainly be considered to be in the low-magnetic-field regime.

We take the result of Lewis and Sondheimer⁵⁵ at room temperature for the Γ_{1C} minimum giving $r = 1.14$ for the purer material where PO scattering is dominant. Wolfe *et al.*⁵⁴ experimentally obtained $r = 1.08$, while Harris and Snyder⁵⁶ determined $r = 1.15$ by a capacitive technique. At higher impurity concentrations where metallic degenerate impurity scattering is present, $r \rightarrow 1$. It would be extremely difficult at band crossover to estimate the value for r since it will be changing as the dominant scattering mechanisms alter in importance.

For the X_{1C} minima, it is probable from our results that PO and equivalent intervalley scattering are the most important, and so the solution of the Boltzmann equation to obtain a relaxation time approximation will be extremely complex and will de-

pend on the relative importance of the two mechanisms. To our knowledge no direct measurements of high- and low-field mobilities have been made on the GaP $\langle 100 \rangle$ minima for a useful comparison. Usually, the equation for the Hall constant in GaP is written as $R_H = -1/ne$. Van der Does de Bye,⁵⁷ however, obtained a minimum value for r of 1.20 for GaP from the Faraday rotation effective mass found by Moss *et al.*⁵⁸ Thus, we could reasonably expect r to increase by at least 5% on transfer from the Γ_{1C} to the X_{1C} minima in GaAs.

A further complication is caused by the fact that the X_{1C} minima have an anisotropic effective mass, and we must multiply r by the factor

$$f(K) = 3K(K+2)/(2K+1)^2,$$

where

$$K = m_t/m_l.$$

Taking Pollak *et al.*¹⁸ and Conwell and Vassell's³⁶ values of $0.23m_e$ and $1.30m_e$ for m_t and m_l , we obtain $f(K) \sim 0.85$. Thus, at 50 kbar, R_H will be approximately 10% below the original atmospheric pressure normalized value for no carrier loss, which is the result we have obtained.

Although accurate values of r in both sets of minima are still largely unknown, we have shown that our result is not surprising. We could reverse the argument to say that our results indicate that the low-field value for r in the GaAs- X_{1C} minima for low-impurity-concentration material in increased 5% from its value in the Γ_{1C} minimum at low magnetic fields.

¹A. R. Hutson, A. Jayaraman, A. G. Chynoweth, A. S. Coriell, and W. L. Feldmann, *Phys. Rev. Letters*, **14**, 639 (1969).

²M. Shyam, J. W. Allen, and G. L. Pearson, *IEEE Trans. Electron. Devices* **ED-13**, 63 (1965).

³Services Electronic Research Laboratory, Baldock, England (private communication).

⁴C. Hilsum and J. Welborn, *J. Phys. Soc. Japan Suppl.* **21**, 532 (1966).

⁵T. Hara and I. Akasaki, *J. Appl. Phys.* **39**, 285 (1968).

⁶A. S. Epstein, *J. Phys. Chem. Solids* **27**, 1611 (1966).

⁷A. R. Hutson, A. Jayaraman, and A. S. Coriell, *Phys. Rev.* **155**, 786 (1967).

⁸J. Lees, M. P. Wasse, and G. King, *Solid State Commun.* **5**, 52 (1967).

⁹W. M. De Meis, thesis, Harvard University Technical Report No. HP-15, 1965.

¹⁰R. A. Stradling and R. A. Wood, *J. Phys. C* **1**, 1711 (1968).

¹¹T. M. Chamberlain and R. A. Stradling, *Solid State Commun.* **7**, 1275 (1969).

¹²Q. H. F. Vrehen, *J. Phys. Chem. Solids* **29**, 129 (1968).

¹³H. Ehrenreich, *Phys. Rev.* **120**, 1951 (1960).

¹⁴C. Hilsum, in *Semiconductors and Semimetals*, edited by R. K. Willardson and A. C. Beer (Academic, New York, 1966), Vol. I.

¹⁵W. E. Spicer and R. C. Eden, *Proceedings of the International Conference on Physics of Semiconductors*, 1968 (Nauka Press, Moscow, 1969), p. 65.

¹⁶J. L. Birman, M. Lax, M. R. London, *Phys. Rev.* **145**, 620 (1966).

¹⁷L. W. James, R. C. Eden, J. L. Moll, and W. E. Spicer, *Phys. Rev.* **174**, 909 (1968).

¹⁸F. H. Pollak, C. W. Higginbottom, and M. Cardona, *J. Phys. Soc. Japan Suppl.* **21**, 20 (1966).

¹⁹W. Paul, *J. Appl. Phys. Suppl.* **32**, 2082 (1961).

²⁰B. B. Kosicki, thesis, Harvard University Technical Report No. HP-19, 1967 (unpublished).

²¹G. D. Pitt, *High Temp. - High Pressure* **1**, 111 (1969).

²²E. J. Moore, *Phys. Rev.* **160**, 607; **160**, 618 (1967).

²³H. Brooks, *Advan. Electron. Electron. Phys.* **8**, 87 (1955).

²⁴R. Mansfield, *Proc. Phys. Soc. (London)* **B69**, 76 (1956).

²⁵G. A. N. Connell, *High Temp. - High Pressure* **1**, 77 (1969).

²⁶E. M. Conwell, *Solid State Phys. Suppl.* **9**, 210 (1967).

²⁷P. N. Butcher, *Rept. Progr. Phys.* **30**, 93 (1967).

²⁸W. Fawcett, A. D. Boardman, and S. W. Swain, *J. Phys. Chem. Solids* **31**, 1963 (1970).

²⁹D. Long, *Phys. Rev.* **120**, 2024 (1960).

³⁰L. W. James, Ph. D. thesis, Stanford University, 1968 (unpublished).

³¹G. D. Pitt, *J. Phys. E* **1**, 915 (1968).

³²H. J. McSkimin, A. Jayaraman, and A. Andreatch, *Jr., J. Appl. Phys.* **38**, 2362 (1967).

³³E. S. Meieran, *J. Appl. Phys.* **36**, 2544 (1965).

³⁴M. S. Abrahams, C. J. Buiochi, and J. J. Tietjen, *J. Appl. Phys.* **38**, 760 (1967).

³⁵For the higher impurity concentrations the value of r can increase (see Appendix) leading to lower values of the conductivity mobility.

³⁶E. M. Conwell and M. O. Vassell, *Phys. Rev.* **166**, 797 (1968).

³⁷I. G. Davies, H. G. B. Hicks, and D. F. Manley (private communication).

³⁸L. R. Weisberg, *J. Appl. Phys.* **33**, 1817 (1962).

³⁹B. R. Gossick, *J. Appl. Phys.* **30**, 1214 (1959).

⁴⁰H. G. B. Hicks and D. S. Manley, *Solid State Commun.* **7**, 1463 (1969).

⁴¹W. Paul, *Proceedings of the International Conference on Physics of Semiconductors, Moscow*, 1968 (Nauka Press, Moscow, 1969), p. 16.

⁴²G. L. Pearson and J. Bardeen, *Phys. Rev.* **75**, 865 (1949).

⁴³H. C. Montgomery, *J. Appl. Phys.* **39**, 2002 (1968).

⁴⁴M. G. Craford, G. E. Stillman, J. A. Rossi, and N. Holonyak, Jr., *Phys. Rev.* **168**, 867 (1968).

⁴⁵N. Holonyak, Jr., C. J. Nuese, M. D. Sirkis, and G. E. Stillman, *Appl. Phys. Letters* **8**, 83 (1962).

⁴⁶B. B. Kosicki, A. Jayaraman, and W. Paul, *Phys. Rev.* **172**, 764 (1968).

⁴⁷C. J. Summers, R. Dingle, and D. E. Hill, *Phys. Rev. B* **1**, 1603 (1970).

⁴⁸T. K. Gaylord and T. A. Rabson, *Phys. Letters* **29A**, 716 (1969).

⁴⁹R. W. Keyes and M. Pollak, *Phys. Rev.* **118**, 1001 (1960).

⁵⁰H. B. Harland and J. C. Woolley, *Can. J. Phys.* **44**, 2715 (1966).

- ⁵¹H. Piller, *J. Phys. Chem. Solids* 24, 425 (1963).
- ⁵²D. Jones and A. H. Lettington, *Solid State Commun.* 7, 1319 (1969).
- ⁵³D. J. Howarth and E. H. Sondheimer, *Proc. Roy. Soc. (London)* 219, 53 (1953).
- ⁵⁴C. M. Wolfe, A. G. Foyt, and W. T. Lindley, *Electrochem. Technol.* 6, 208 (1968).
- ⁵⁵B. F. Lewis and E. H. Sondheimer, *Proc. Roy. Soc. (London)* 227, 241 (1955).
- ⁵⁶J. S. Harris and W. L. Snyder, *Solid State Electron.* 12, 337 (1969).
- ⁵⁷J. A. W. Van der Does de Bye and R. C. Peters, *Philips Res. Rept.* 24, 210 (1969).
- ⁵⁸T. S. Moss, A. K. Walton, and B. Ellis, *Proceedings of the International Conference on the Physics of Semiconductors, Exeter, 1962* (The Institute of Physics and the Physical Society, London, 1962), p. 295.